A 13.56MHz Fully Integrated 91.8% Efficiency Single-Stage Dual-Output Regulating Voltage Doubler for Biomedical Wireless Power Transfer

Lu, Tianqi ; Chang, Zu Yao; Jiang, Junmin; Makinwa, Kofi; Du, Sijun

DOI
10.1109/CICC57935.2023.10121186

Publication date
2023

Document Version
Final published version

Published in
Proceedings of the 2023 IEEE Custom Integrated Circuits Conference (CICC)

A 13.56MHz Fully Integrated 91.8% Efficiency Single-Stage Dual-Output Regulating Voltage Doubler for Biomedical Wireless Power Transfer

Tianqi Lu[1], Zu-yao Chang[1], Junmin Jiang[2], Kofi Makinwa[1], and Sijun Du[1]

[1]Delft University of Technology, Delft, the Netherlands

[2]Southern University of Science and Technology, Shenzhen, China

2023 IEEE Custom Integrated Circuits Conference (CICC) | 979-8-3503-9948-6/23/$31.00 ©2023 IEEE | DOI: 10.1109/CICC57935.2023.10121186

Dual-output regulating rectifier is highly desired in wireless power transfer (WPT) for sub-100mW bioimplants. Such rectifiers perform voltage rectification and dual-output regulation simultaneously, thus avoiding post DC-DC conversions and cascaded power losses [1-4]. However, the conventional dual-output structure suffers from a low voltage conversion ratio (VCR) (<1) due to the full bridge rectifier (FBR) topology (Fig. 1), severely limiting the receiver operation when wireless link condition varies [1-2]. In order to extend the operational range without increasing the power demand from the transmitter, [3] presents a charge-pump based dual-output rectifier; however, it uses 10 power transistors (PTs) and 8 off-chip capacitors, degrading the power conversion efficiency (PCE) and increasing the integration cost. Alternatively, the current-mode dual-output rectifier can realize a VCR higher than 1, but the output power is limited to less than 10mW [4], which is insufficient for advanced bioimplants. In this work, a 13.56MHz single-stage dual-output voltage doubler (DOVD) is proposed to address the above limitations, which employs only two PTs and a fully integrated design. It can achieve a peak VCR of 1.78 and outputs power up to 81mW with a 91.8% peak PCE.

The proposed DOVD consists of two PTs, S_P and S_N, and two output capacitors, C_{L1} and C_{L2}, in the power stage. Fig. 1 shows the working principle of the DOVD with 4-phase operation. When both outputs, V_{DC1} and V_{DC2}, need to be charged, the DOVD operates in Φ_1, where both S_P and S_N are enabled to deliver power to C_{L1} and C_{L2}, respectively. When only V_{DC1} needs to be charged, the DOVD switches to Φ_2, where S_N is disabled so that only C_{L1} is charged. In Φ_3, S_P is disabled, and the DOVD charges C_{L2} through S_N to build V_{DC2}. Due to the stack topology of C_{L1} and C_{L2}, V_{DC1} also increases slightly when C_{L2} is charged, but this can then be compensated by the controller, as will be explained later. When both V_{DC1} and V_{DC2} do not require energy from the AC input, the DOVD enters Φ_4, the freewheeling phase, where both S_P and S_N are disabled.

Fig. 2 presents the architecture of the proposed DOVD with controller and the operation principle of the dual-output regulation. S_P (or S_N) is controlled by the delay-compensated comparator CMP_P (or CMP_N) through the gate driver $Driver_P$ (or $Driver_N$), functioning as a power-efficient active diode when enabled. To eliminate the dual-output cross-regulation issue, the parallel pulse frequency modulation (PPFM) controller is proposed, regulating V_{DC1} and V_{DC2} in two distinct hysteresis windows independently. If V_{DC1} (or V_{DC2}) reaches the lower hysteresis threshold, S_P (or S_N) will be enabled by signal EN_P (or EN_N) to charge C_{L1} (or C_{L2}). When V_{DC1} (or V_{DC2}) reaches the upper hysteresis threshold, S_P (or S_N) will be disabled. Selectively enabling the two PTs results in the 4-phase operation. In the freewheeling phase (Φ_4), an over-voltage protection block is activated by the controller (S_{OVP}) to limit the open-circuit V_{AC}.

Fig. 3 shows the circuit implementation of the PPFM controller. To regulate V_{DC1} and V_{DC2}, the controller firstly employs two op-amp comparators (CMPs) to compare the divided versions of V_{DC1} and V_{DC2} with a reference voltage V_{REF} generated on chip. The hysteresis window for V_{DC1} (or V_{DC2}) regulation is defined by the positive feedback resistor R_5 (or R_6) and the resistive voltage divider. The control signals EN_P, EN_N and S_{OVP} are then derived from the CMP outputs, V_{FB1} and V_{FB2}, synchronized with the CLK signal (recovered from V_{AC}). Therefore, EN_P, EN_N and S_{OVP} will not change until V_{AC} roughly equals V_{DC2}, resulting in a zero-voltage phase switching avoiding switching noise and efficiency degradation.

When the DOVD works in Φ_2 (or Φ_3) where S_N (or S_P) is disabled, V_{AC} can level up during the half period without resistive loading. The amplitude of V_{AC} can easily go lower than $-|V_{TH,N}|$ (or higher than $(V_{DC1}+|V_{TH,P}|)$). To avoid the undesired channel conduction in S_N (or S_P), $Driver_N$ (or $Driver_P$) is designed to clamp V_{GN} (or V_{GP}) to the adaptive biasing V_{MIN} (or V_{MAX}), which tracks the minimum (or maximum) voltage in the system, when S_N (or S_P) is disabled, as shown in Fig. 3.

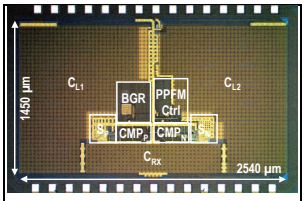

Die micrograph.

To drive S_P (or S_N) properly at 13.56 MHz, the delays in CMP_P (or CMP_N) and $Driver_P$ (or $Driver_N$) need to be compensated, or reverse currents and extra conduction losses could pop up. Therefore, CMP_P and CMP_N are designed to be switched-biased push-pull comparators with adaptive delay compensation blocks [5] (Fig. 3). By sampling V_{AC} at the turn-on/off moment of S_P (or S_N) and comparing it to V_{DC1} (or GND) by the error amplifier, the gate-driving delay can steer the feedback loop tuning the bias current in the push-pull comparator, then aligning the turn-on/off timing of S_P (or S_N). The coupling/loading-insensitive delay compensation results in a high PCE. Moreover, shield switches are used to introduce V_{MIN} (or V_{MAX}) into CMP_N (or CMP_P), ensuring robust transistor shutoff when CMP_N (or CMP_P) is disabled in Φ_2 (or Φ_3).

The proposed DOVD was fabricated in the 180nm BCD process, occupying a chip area of 0.4/3.68mm^2 with/without capacitors. The on-chip resonance capacitor C_{RX} (518pF) is implemented by MIM capacitors; C_{L1} and C_{L2} are MOS/MIM stacking capacitors (3.9nF each). Fig. 4 shows the measured steady state operation waveforms and load transient waveforms of the DOVD. In the steady state, V_{AC} amplitude changes dramatically, notifying 4-phase operation, which can also be verified by EN_P and EN_N. V_{DC1} and V_{DC2} are regulated at 3.6V and 1.8V, respectively, within preset hysteresis windows. The load transient waveforms were measured when R_{L1} was changed between 500Ω and 4kΩ in both directions and R_{L2} was kept equal to 2kΩ. No voltage undershoot/overshoot is observed at the transient moments, and more importantly, the cross-regulation issue is not observable because, by the nature of the proposed PPFM controller, the response of load transient is theoretically instantaneous and only determined by the preset hysteresis windows [6].

The top half of Fig. 5 shows the self-startup setting and the measured self-startup operation of the DOVD. During startup, the DOVD is forced to work as a passive voltage doubler by diode-connecting S_P and S_N. A V_{TH}-based startup detector is designed to activate the DOVD mode when V_{DC1} reaches $V_{TH,ST}$ (3V). The bottom half of Fig. 5 shows the measured VCR and PCE results of the DOVD. A VCR larger than 1 is easily obtained at V_{DC1}, thanks to the voltage doubler topology. The peak VCR reaches 1.78 when R_{L1}=R_{L2}=4kΩ. Because only two PTs, with gate-driving delay compensated, are employed in the power stage, a high PCE is attained. The peak PCE reaches 91.8% when the total output power P_{OUT} is 33.5mW, and the PCE keeps higher than 87% when P_{OUT} is larger than 30mW.

Fig. 6 compares the proposed DOVD with state-of-the-art regulating rectifiers. This work is the only one simultaneously achieving: 1) dual-output regulation, 2) higher-than-1 VCR, 3) up-to-81mW available P_{OUT}, while keeping a state-of-the-art PCE. By fully Integrating the resonance and output capacitors on chip, this work also achieves the smallest receiver volume (1.97mm^3) and the highest power density (41.12mW/mm^3) among the designs in the table.

Acknowledgement:

The authors would like to acknowledge EUROPRACTICE for MPW and design tool support.

References:

[1] F. Marefat *et al.*, ISSCC, Feb. 2020.

[2] F. -B. Yang *et al.*, VLSI, Jun. 2022.

[3] Z. Xue *et al.*, CICC, Apr. 2018.

[4] H. S. Gougheri *et al.*, TBioCAS, vol. 13, no. 5, Oct. 2019.

[5] L. Cheng *et al.*, JSSC, vol. 51, no. 3, Mar. 2016.

[6] J. Tang *et al.*, ISSCC, Feb. 2021.

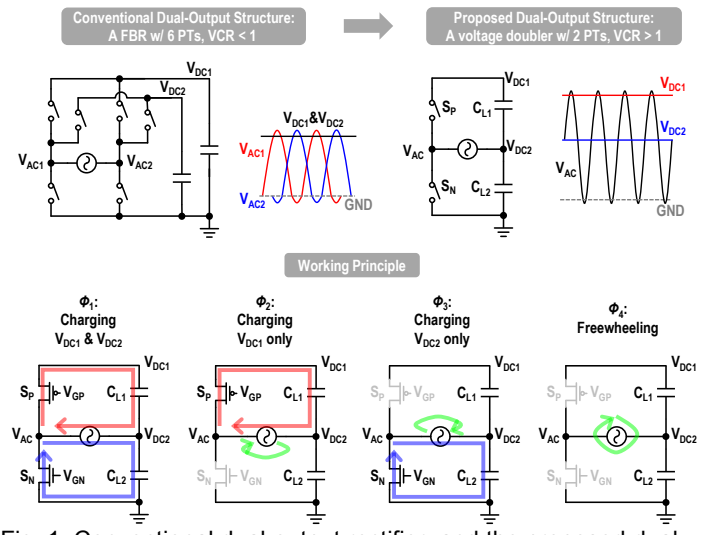

Fig. 1. Conventional dual-output rectifier, and the proposed dual-output voltage doubler structure and its working principle.

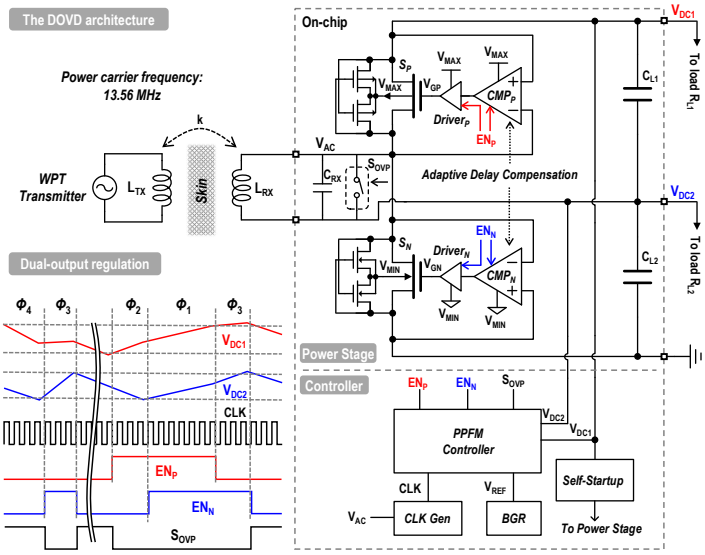

Fig. 2. Architecture of the proposed DOVD with controller, and the operation principle of its dual-output regulation.

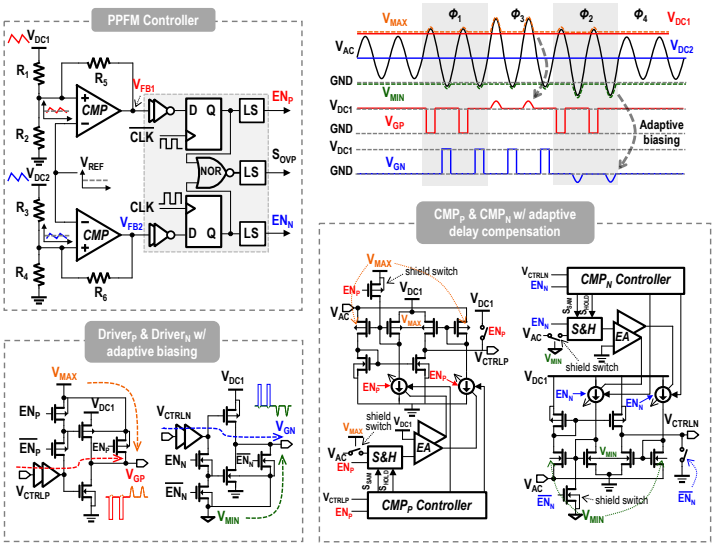

Fig. 3. Circuit implementations of the PPFM controller, the PT drivers and the PT driving comparators.

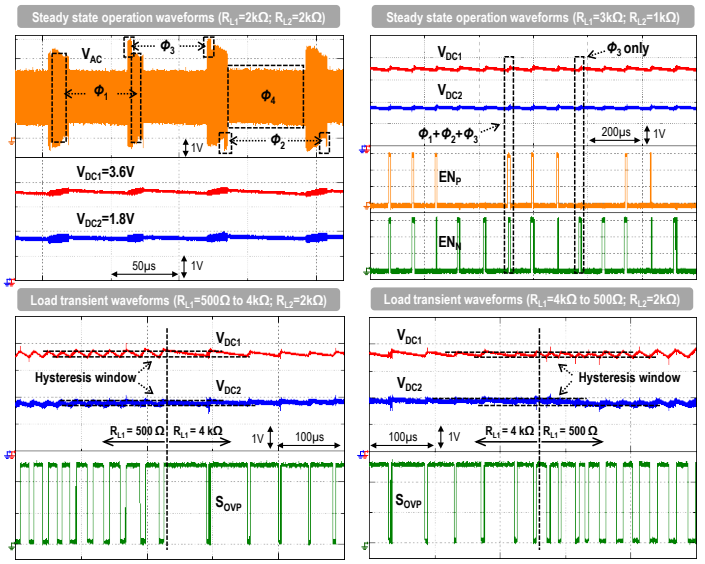

Fig. 4. Measured steady-state waveforms and load transient responses.

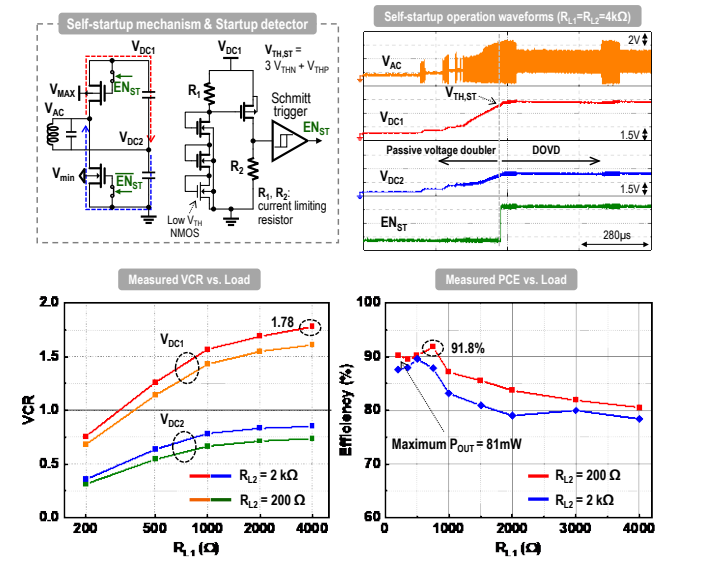

Fig. 5. The schematic and measured operation waveforms of the self-startup setting, and the measured VCR and PCE results.

	This work	[1] ISSCC 2020	[2] VLSI 2022	[3] CICC 2018	[4] TBCAS 2019
Technology	180-nm BCD	180-nm CMOS	180-nm CMOS	180-nm CMOS	350-nm CMOS
Input frequency	13.56 MHz	2 MHz	6.78 MHz	13.56 MHz	1 MHz
Chip area	0.4 mm² (w/o caps); 3.68 mm² (w/ caps)	6 mm²	2.32 mm²	0.66 mm²	2.7 mm²
Receiver topology	Dual-output regulating voltage doubler	Dual-output full-bridge rectifier	Dual-output full-bridge rectifier	Charge-pump based dual-output rectifier	Current mode dual-output rectifier
# of power transistors	2	6	6	10	5
Fully integrated (off-chip components)	Yes	No (2 capacitors)	No (2 capacitors)	No (8 capacitors)	No (2 capacitors)
Receiver volume*	1.97 mm³	5.64 mm³	3.44 mm³	8.56 mm³	3.66 mm³
Output voltages (# of regulated outputs)	1.8 V, 3.6 V (2)	1.5 V, 2.5 V (2)	3.7 V, 5 V (2)	1.7 V, 2.75 V (2)	2.6 V, 3.9 V (2)
Peak VCR	1.78 ($R_{L1,2}$=4kΩ)	0.83**	0.85**	2.75	4.88**
Maximum P_{OUT}	81 mW ($R_{L1,2}$=200Ω)	65 mW	300 mW	10 mW	45 mW
Peak PCE	91.8% (@ 33.5mW)	90.75% (@ 65 mW)	91.7% (@ 200** mW)	79% (@ 7.1 mW)	75.3% (@ 4.7 mW)
Power density***	41.12 mW/mm³	11.52 mW/mm³	8.02 mW/mm³	1.17 mW/mm³	12.29 mW/mm³

*Assuming off-chip capacitors have the most compact cases on PCB based on their values.

**Estimated from plotted data.

***Calculated by $\frac{Maximum\ P_{OUT}}{Receiver\ volume}$

Fig. 6. Performance summary of the proposed DOVD and comparison to state-of-the-art designs.